Original Article

使用表面掃掠技術來測量與評估漸進多焦點鏡片

Measurement and Evaluation of Progressive Addition Lenses by Surface Sweeping Technique

黃敬堯 Ching-Yao Huang*
Department of Optometry, College of Nursing and Health Sciences, Da-Yeh University

摘要：

本研究是使用一種具有五軸快速表面掃掠功能的非光學精密三次元量床來測量與評估三種不同鏡片設計(前面累進、後面累進、雙面自由曲面)的漸進多焦點鏡片的光學性質。鏡片前後表面的幾何高度可被測量出來，並以Zernike多項式組合形態來表示其表面形狀。鏡片的前後各別表面及其組合後的光學性質能透過MATLAB程式計算得到，並以等價球面度數、散光度數，及高階像差分佈圖呈現。如所預期，所有漸進多焦點鏡片的光學性質都直接與其鏡片設計種類及近加入度數有關。此外，由此五軸快速表面掃掠功能的三次元量床所花的每面平均測量時間已有效地縮短至5分鐘以下，此結果顯示非光學的表面掃掠測量方法是有可能比得上光學的測量方法。

Abstract:

This study measures and evaluates optical properties of progressive addition lenses (PALs) with three types of lens designs (front progressive, back progressive, freeform both surfaces) by a non-optical precision surface sweeping coordinate measuring machine (CMM) with a five-axis probing system. The front and back surface heights were physically measured, and surface shapes were represented as the sum of Zernike polynomials. The optical properties of each surface and their combination were calculated with custom MATLAB programs in terms of contour plots of spherical equivalent, astigmatism, and higher-order aberrations (HOAs). As expected, optical properties of all PALs are directly related to their lens designs and add powers. The average measuring time spent by the surface sweeping CMM method has been greatly reduced to less than 5 minutes, which makes it possible to be comparable to the optical measuring methods.

Keywords: progressive addition lenses, coordinate measuring machine, surface sweeping, Zernike polynomials, lens design, add power

TOVS, 2016; 1(2): 50-60

*Corresponding author: 黃敬堯 **Ching-Yao Huang**
Department of Optometry, College of Nursing and Health Sciences, Da-Yeh University, No. 168, University Rd., Dacun, Changhua 51591, Taiwan, R.O.C.
E-mail: **cyhuang@mail.dyu.edu.tw**

Introduction

The optical characteristics of progressive addition lenses (PALs) have been extensively measured and evaluated by the optical methods over the past 60 years, including lensometry [1-5], interferometry [6-11], and wavefront aberrometry [12-16]. Through direct optical measurements, the key features of PALs have been efficiently and systematically revealed, which consist of a vertical increase in spherical power from the upper distance vision zone to the lower near vision zone of the lens, a lateral increase in unwanted astigmatism to either side of the progressive corridor, and a concentrated distribution of higher-order aberrations (HOAs) along the progressive corridor area and around the near vision zone. However, the types of PALs with contemporary freeform lens designs (front progressive, back progressive, or freeform both surfaces) can not be fully verified by these optical methods.

Recent research has demonstrated that both the optical properties and lens types of PALs can be evaluated by direct measurement of surface shape via a conventional coordinate measuring machine (CMM) with a touch trigger point-type probe scan, which is an indirect, non-optical measuring method [16-21]. However, one major disadvantage when applying this measuring technique is the long measuring time compared with those spent in the optical methods. In general, the measuring time is less than 2 minutes for commercial optical measuring equipment but it takes about 16 hours for 12,100 measurements using the standard CMM touch trigger method to yield similar measurement density to the optical method (one data point per 0.5 mm) [16]. This time-consuming problem really hinders the application of CMM in the measurement of PALs.

Fortunately, with the development of CMM technology, the measuring system has been greatly improved from a conventional touch trigger point-type method to a three-axis continuous scan-type system.

A comparison study showed that the optical properties of PALs measured by the three-axis continuous scan-type CMM are similar to those by the traditional touch trigger point-type CMM, and the scan can shorten more measuring time, down to 30 minutes per surface scan [22]. Recently, a more advanced CMM with a revolutionary measuring head and sweeping probe system is created, which can gather large quantities of accurate inspection data at ultra-high scanning speeds with five-axis motion capability [23-27]. This new measuring technique makes it an invaluable and unique probing system and enables users to achieve previously unobtainable level of inspection.

The tip sensing technology used in the five-axis probing system is specifically designed to enable ultra-fast scanning, reduce the scanning forces and minimize stylus wear. There is an enclosed laser directed on to a reflector at the stylus tip. When the stylus is not deflected, the paths of transmitted and reflected laser beam are the same. As the stylus touches the part and bends, the reflector is displaced and the altered return path of the laser beam is then sensed by a position sensing detector (PSD) which provides signal outputs in the three probe axes and converted into x, y, z signals by the calibration routine. Then, the exact tip position of the stylus is identified because the reflector and stylus ball are close together. A schematic setup of the tip sensing technology is shown in Fig. 1. These features provide it with capability to scan at a speed of 500 mm/s with 4000 points per second acquisition rate. Additionally, the actual force that the probe imparts on the component is very less and is in the range of 0.05 N and 0.25 N. This is order of magnitude lower than the force imparted by traditional spring based probes. This feature makes it suitable for choices where more force cannot

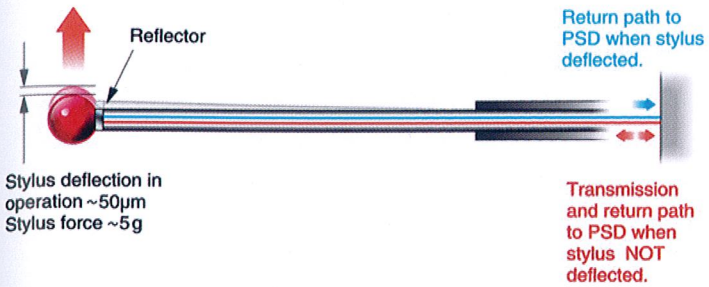

Fig. 1. A schematic setup of the tip sensing technology [27].

be imparted on object, optical lenses are being one of them.

Therefore, it is of great interest to apply tip sensing technology to measure and evaluate PALs not only for the consideration of accuracy of optical properties of PALs but also for the further reducing measuring time. In this study, PALs were measured by an advanced precision CMM with a surface sweeping scan design and five-axis probing system to evaluate optical properties. Measuring time was also compared with those measured by the other scanning type of CMMs.

Methods

A. Materials

Nine sets of contemporary freeform PALs from six leading manufacturers (Asahi-Lite, Essilor, Hoya, Nikon, Seiko, and Zeiss) were selected for comparison of optical properties. Each set of PALs had plano distance power and three add powers (+1.00 D, +2.00 D, +3.00 D). All were left lenses and plastic CR-39 (n=1.50). Among these tested PALs, three types of lens designs can be classified and compared. The first type was a molded progressive front surface with a freeform single-power back surface (Hoya Summit CD and Zeiss GT2). The second type was a molded spherical front surface with a freeform progressive back surface (Nikon Presio Advance, Asahi-Lite Standard, Zeiss Asiana, Seiko Synergy X). The third type was freeform on both surfaces (Varilux Comfort, Nikon Presio Power, and Hoya FD). The lenses had comparable base curves, fitting cross locations, and corridor lengths, as shown in Table 1.

Table 1. Progressive addition lenses used in this study

Design Type	Lens	Base Curve (D)	Corridor Length (mm)	Fitting Cross (mm)
Molded progressive front surface, Freeform single-power back surface	Hoya Summit CD (F1)	4.25	11	4
	Zeiss GT2 (F2)	4.75	10	4
Molded spherical front surface, Freeform progressive back surface	Nikon Presio Advance (B1)	3.50	12	2
	Asahi-Lite Standard (B2)	4.00	11	4
	Zeiss Asiana (B3)	5.00	10	6
	Seiko Synergy X (B4)	4.25	10	2
Freeform both surfaces	Varilux Comfort (D1)	4.25	11	4
	Nikon Presio Power (D2)	3.50	12	2
	Hoya FD (D3)	4.50	11	4

B. Measuring Equipment

Surface height measurement of PALs was conducted by horizontally sweeping across the lens with a precision coordinate measuring machine (Leader NC-787) with a five-axis probing system (Renishaw, REVO). The stylus diameter and length are 6 mm and 10 mm, respectively. The resolution of displacement was about 3 μm. Both front and back surfaces of the lens were measured to derive the full optical properties of the PALs. The surface sweeping CMM with REVO five-axis probing system is shown in Fig. 2.

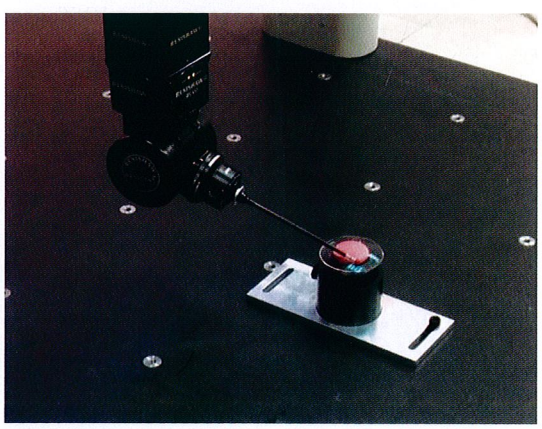

Fig. 2. The precision surface sweeping CMM with REVO five-axis probing system.

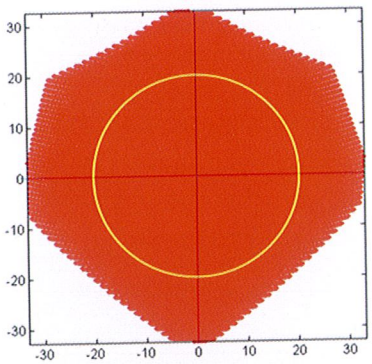

Fig. 3. The surface swept area in the PAL and the evaluated zone within 40-mm diameter (yellow circle).

The lens was measured on a grid of points (x, y) spaced about 0.05 mm apart or about 400 measured points per square millimeter to produce data files that consist of (x, y, z) positions. That measurement density yields about 65,000 samples per surface. These data were saved as a text file and subsequently imported into MATLAB for analysis. The analysis diameter of all PALs was 40 mm. The surface swept area in the PAL and the evaluated zone within 40-mm diameter (yellow circle) are shown in Fig. 3.

Each lens was particularly oriented to make the axis of the coma component of the freeform surface vertical. For measuring the other surface, the lens was flipped around this vertical meridian. For analysis, the measured data were flipped back, so that corresponding points on front and back surfaces superimposed. A detailed description of the measuring process has been described elsewhere [16-18, 28].

The optical properties of the tested PALs including spherical equivalent power (M), astigmatism (J), and higher-order aberrations (HOAs) were calculated for each surface and for the combination of both surfaces and illustrated in the standard format of contour plots generated with custom MATLAB programs [16-18]. In this study, only the optical properties in lens area of 40-mm diameter were examined.

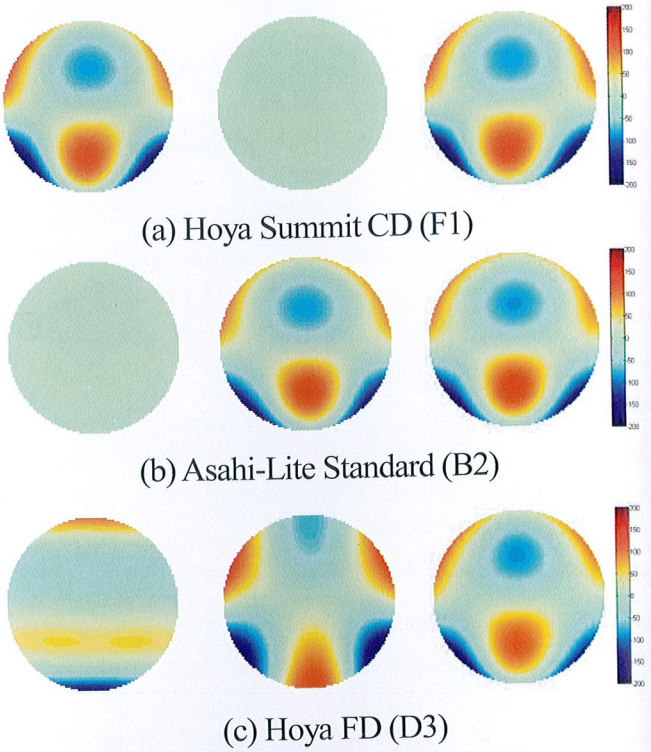

(a) Hoya Summit CD (F1)

(b) Asahi-Lite Standard (B2)

(c) Hoya FD (D3)

Fig. 4. Front surface height (left), back surface height (middle) and thickness (right) profile in micrometers of three PALs with different lens design (higher order terms only) (a) Hoya Summit CD (F1), (b) Asahi-Lite Standard (B2), (c) Hoya FD (D3). The add power is +3.00 D.

Results and Discussion

A. Optical Properties of PALs

1. Surface Height and Thickness

Figure 4 shows the front and back surface height profiles and thickness profile resulting from the combination of the two surface heights in three representative PALs with different lens design and a +3.00-D add. All profiles are generated from the higher order terms only because the spherocylindrical (second-order) terms are essentially irrelevant to the progressive power of the lens [17, 18], which is illustrated by the uniform color with zero height.

It is obvious that the front and back surface height profiles among these three lens designs are different. The Hoya Summit CD shows a freeform front surface and a spherocylindrical back surface, consistent with the single front progressive lens design

The Asahi-Lite Standard shows spherocylindrical on the front surface and freeform on the back surface, consistent with the single back progressive lens deign. However, the Hoya FD shows totally different lens design form Hoya Summit CD and Asahi-Lite Standard, which has freeform on both surfaces. The front surface is freeform designed with the third-order Zernike terms of both coma and trefoil. The back surface is freeform designed with predominantly the third-order Zernike term of trefoil [18].

Although the surface height profiles of front and back surfaces are different for these three representative PALs with different lens design, the thickness from the combination of the two surfaces all look similar. They all show relatively concave portions for distance vision and relatively convex portions for near vision. The other PALs with different add powers and lens designs also show similar results, except of the Varilux Comfort and Nikon Presio Power with different freeform design on both surfaces.

2. Spherical Equivalent Power and Astigmatism

Figure 5 and 6 show contour plots of the whole-surface spherical equivalent power (M) and astigmatism (J) of these three representative PALs with a +3.00-D add on the front, back, and combined surface, respectively. The contour lines shown in the plots are separated by 0.50 D. As expected in any PAL, the overall spherical equivalent power increases along the progressive corridor, and the astigmatism increases laterally from the vertical midline shown in the combined surface profile.

The negative sphere values in the upper portion of these PALs is caused by the second-order Zernike coefficient (defocus) being initially set to zero in the calculation of surface height, thus making the average spherical equivalent power of the lens close to plano [18]. However, the add power is still about +3.00 D from the distance zone to the near zone, consistent with the lens specifications of plano distance power with a +3.00-D add.

According to the power distributions on the front and back surface among these three PALs in Fig. 5 and 6, it also clearly shows that Hoya Summit CD has progressive front surface design, Asahi-Lite Standard has progressive back surface design, and Hoya FD has a freeform design on both surfaces, corresponding to the surface height profiles shown in Fig. 4. Moreover, it is interesting to note that the profiles of the spherical equivalent power and astigmatism in the combined surface of these three PALs also look similar, which is again consistent with the thickness profile shown in Fig. 4.

However, the amount of unwanted astigmatism in the Hoya FD with freeform

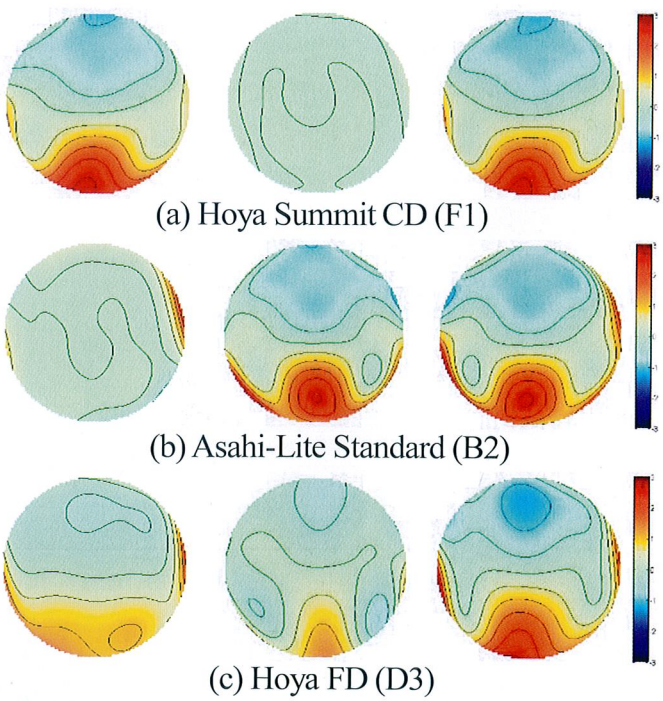

(a) Hoya Summit CD (F1)

(b) Asahi-Lite Standard (B2)

(c) Hoya FD (D3)

Fig. 5. Contour plots of spherical equivalent power of three PALs with different lens design on the front (left), back (middle), and combined surface (right) (a) Hoya Summit CD (F1), (b) Asahi-Lite Standard (B2), (c) Hoya FD (D3). The add power is +3.00 D.

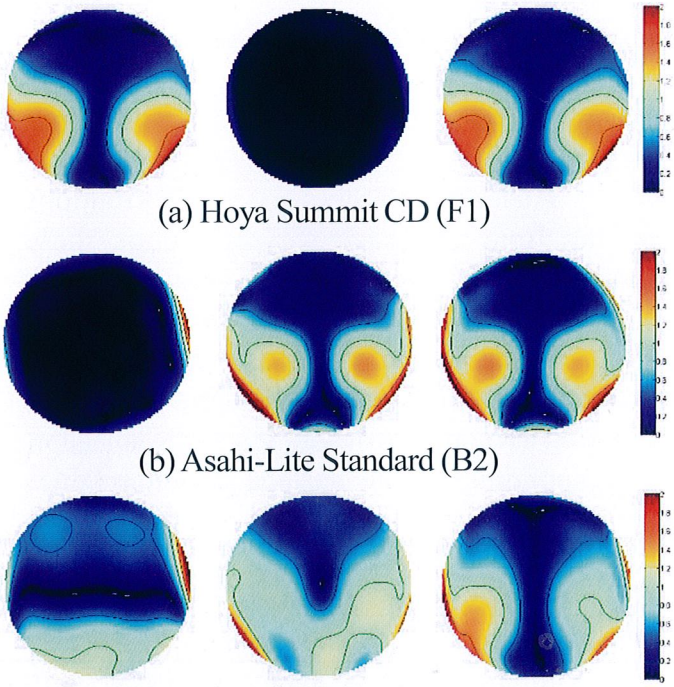

(a) Hoya Summit CD (F1)

(b) Asahi-Lite Standard (B2)

(c) Hoya FD (D3)

Fig. 6. Contour plots of astigmatism of three PALs with different lens design on the front (left), back (middle), and combined surface (right) (a) Hoya Summit CD (F1), (b) Asahi-Lite Standard (B2), (c) Hoya FD (D3). The add power is +3.00 D.

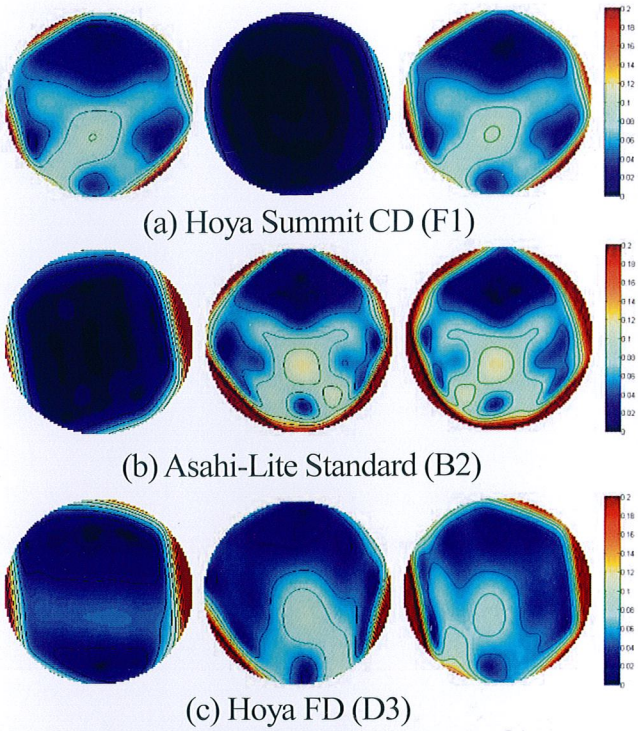

(a) Hoya Summit CD (F1)

(b) Asahi-Lite Standard (B2)

(c) Hoya FD (D3)

Fig. 7. Contour plots of higher order aberrations of three PALs with different lens design on the front (left), back (middle), and combined surface (right) (a) Hoya Summit CD (F1), (b) Asahi-Lite Standard (B2), (c) Hoya FD (D3).

both surface lens design seems to be about 0.50 D less than that in the Hoya Summit CD with single front progressive or the Asahi-Lite Standard with single back progressive surface lens design. This indicates that the unwanted astigmatism is strongly affected by the lens designs. Obviously, the most intriguing design is the Hoya FD, which uses sophisticated surface designs on the front and the back. Fig. 4 has demonstrated that the freeform front surface results from the third-order Zernike terms of both coma and trefoil and the trefoil is the dominant component on the freeform back surface, which might explain for the lower unwanted astigmatism. The PALs with different add powers and the other six PALs belonging to different design groups also show similar results. The detailed systematical comparisons are described in the next section.

3. Higher Order Aberrations (HOAs)

Figure 7 shows contour plots of the higher order aberrations (HOAs) in root mean square (RMS) error through a 4.5-mm pupil for the front, back, and combined surface in these three representative PALs with a +3.00-D add, respectively. It is obvious that the freeform surface of each PAL is responsible for the HOAs, whereas the spherocylindrical surfaces show a low level of HOAs close to zero. As expected in any PAL, the RMS of HOAs tends to be higher in the progressive corridor area and the area surrounding the near power zone, corresponding to the variation in spherical equivalent power

and astigmatism across the lens.

As expected, coma and trefoil are the dominant high-order terms present in PALs regardless of the lens design. However, the amount of HOAs varies with lens design. The maximum RMS of HOAs occurred within the corridor area and is about 0.10 μm for the PAL with single front progressive lens design (Hoya Summit CD) and 0.12 μm for the PAL with back progressive lens design (Asahi-Lite Standard) at a +3.00-D add. The PAL with freeform on both surfaces (Hoya FD) shows less HOAs compared with the above two PALs— about 0.09 μm. The possible reason might be due to the sophisticated surface design on the front and the back to yield lower HOAs, similar to that described in the aforementioned unwanted astigmatism.

B. Effect of Add Power and Lens Design

The effect of add power and lens designs on the optical properties of PALs can be illustrated in terms of the maximum power rate change along the corridor, minimum 1.00-DC corridor width, and HOAs. Table 2 to 4 show comparison of the maximum power rate, HOAs, and minimum 1.00-DC corridor width in nine PALs with add powers of +1.00 D, +2.00 D, and +3.00 D for a measurement diameter of 40 mm.

It clearly shows that the Hoya Summit CD, and Zeiss GT2 have progressive power changes on the front surface, whereas the Nikon Presio Advance, Asahi-Lite Standard, Zeiss Asiana, and Seiko Synergy X have progressive power changes on the back surface. It is interesting to note that the Varilux Comfort, Nikon Presio Power, and Hoya FD have unequal progressive power changes on both surfaces which make them belong to the freeform both-surface lens design. All PALs are consistent with the manufacturers' lens designs.

1. Power Rate

Figure 8 shows comparison of the average maximum power rate among PALs with different add powers and lens designs. It is apparent that the average maximum power rate increases with increasing add power regardless of the lens design. It also shows that PALs with freeform both-surface lens design tend to have lower power rate than the other two single-surface progressive lens designs by about 0.01 to 0.04 D/mm, especially at higher add power. Moreover, PALs with the back progressive lens design tend to have the highest average maximum power rate up to 0.17 D/mm for an add power of +3.00 D. In comparison, the add power plays a more important role than the lens design in determining power rate.

2. Width of Corridor

Figure 9 shows comparison of the average minimum 1.00-DC corridor width among PALs with different add powers and lens designs. It is apparent that the average minimum 1.00-DC corridor width dramatically decreases with increasing add power regardless of the lens design. It also shows that PALs with freeform both-surface lens design have slightly wider corridors than the single-surface progressive lens designs by about 1.0 to 3.4 mm. Moreover, PALs with the back progressive lens design tend to show the narrowest corridor, corresponding to the tendency in the power rate. Fig. 9 clearly indicates that the add power plays a more important role than the lens design on the width of corridor.

3. Higher Order Aberrations (HOAs)

Figure 10 shows a comparison of the average maximum HOAs in RMS error among PALs with different add powers and lens designs. It is apparent that the average maximum HOAs increase with increasing add power regardless of the lens design. Similarly, it also shows that PALs with freeform both-surface lens

Table 2. Comparison of the maximum power rate, HOAs, and minimum corridor width in nine PALs with add power of +1.00 D for a lens diameter of 40 mm

PALs	Maximum power rate, D/mm			Maximum HOAs,μm			Minimum 1.00-DC corridor width, mm
	Front surface	Back surface	Combined surface	Front surface	Back surface	Combined surface	
Hoya Summit CD (F1)	0.054	0.007	0.061	0.034	0.005	0.037	17.9
Zeiss GT2 (F2)	0.038	0.008	0.045	0.037	0.010	0.041	29.0
Nikon Presio Advance (B1)	0.025	0.059	0.054	0.017	0.041	0.041	17.6
Asahi-Lite Standard (B2)	0.004	0.065	0.069	0.004	0.042	0.043	23.9
Zeiss Asiana (B3)	0.011	0.036	0.051	0.010	0.039	0.046	27.8
Seiko Synergy X (B4)	0.010	0.058	0.065	0.012	0.040	0.045	16.4
Varilux Comfort (D1)	0.045	0.025	0.044	0.031	0.022	0.039	28.4
Nikon Presio Power (D2)	0.057	0.025	0.071	0.046	0.018	0.054	10.1
Hoya FD (D3)	0.051	0.005	0.041	0.035	0.044	0.054	35.8

Table 3. Comparison of the maximum power rate, HOAs, and minimum corridor width in nine PALs with add power of +2.00 D for a lens diameter of 40 mm

PALs	Maximum power rate, D/mm			Maximum HOAs,μm			Minimum 1.00-DC corridor width, mm
	Front surface	Back surface	Combined surface	Front surface	Back surface	Combined surface	
Hoya Summit CD (F1)	0.098	0.007	0.094	0.067	0.003	0.066	7.8
Zeiss GT2 (F2)	0.064	0.009	0.070	0.069	0.008	0.070	7.5
Nikon Presio Advance (B1)	0.010	0.111	0.112	0.005	0.077	0.075	6.9
Asahi-Lite Standard (B2)	0.002	0.115	0.122	0.003	0.084	0.085	5.8
Zeiss Asiana (B3)	0.003	0.075	0.083	0.005	0.085	0.088	4.9
Seiko Synergy X (B4)	0.005	0.114	0.118	0.033	0.079	0.091	6.6
Varilux Comfort (D1)	0.089	0.043	0.097	0.067	0.023	0.076	6.9
Nikon Presio Power (D2)	0.098	0.037	0.109	0.079	0.013	0.084	6.0
Hoya FD (D3)	0.068	0.016	0.079	0.047	0.074	0.061	10.4

Table 4. Comparison of the maximum power rate, HOAs, and minimum corridor width in nine PALs with add power of +3.00 D for a lens diameter of 40 mm

PALs	Maximum power rate, D/mm			Maximum HOAs,μm			Minimum 1.00-DC corridor width, mm
	Front surface	Back surface	Combined surface	Front surface	Back surface	Combined surface	
Hoya Summit CD (F1)	0.142	0.007	0.149	0.101	0.004	0.103	4.6
Zeiss GT2 (F2)	0.126	0.004	0.129	0.115	0.010	0.110	4.0
Nikon Presio Advance (B1)	0.003	0.165	0.168	0.004	0.113	0.113	4.3
Asahi-Lite Standard (B2)	0.006	0.184	0.188	0.007	0.122	0.121	3.9
Zeiss Asiana (B3)	0.005	0.145	0.152	0.008	0.122	0.125	3.4
Seiko Synergy X (B4)	0.026	0.157	0.179	0.025	0.108	0.116	4.6
Varilux Comfort (D1)	0.113	0.040	0.123	0.089	0.020	0.090	5.7
Nikon Presio Power (D2)	0.133	0.041	0.139	0.109	0.019	0.114	4.5
Hoya FD (D3)	0.068	0.054	0.124	0.049	0.096	0.087	5.8

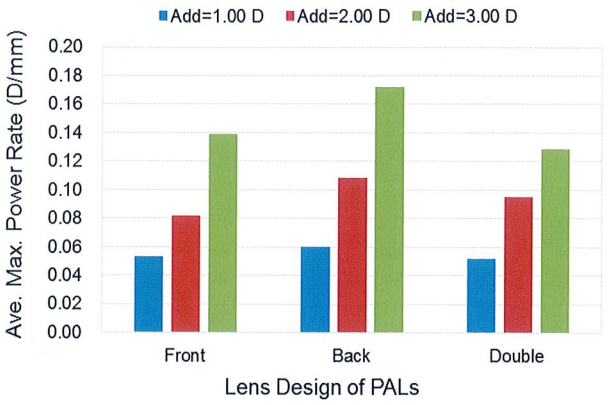

Fig. 8. Effect of add power and lens design on the maximum power rate of PALs.

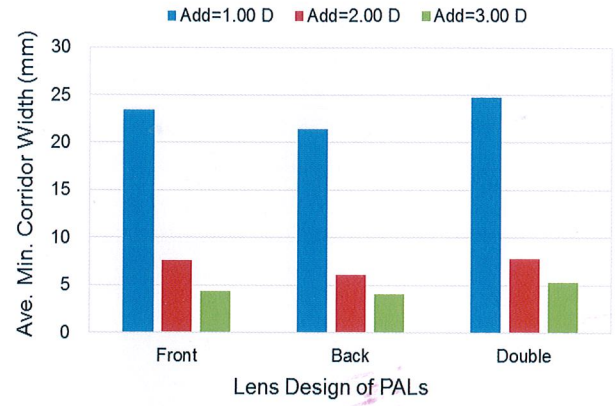

Fig. 9. Effect of add power and lens design on the width of corridor of PALs.

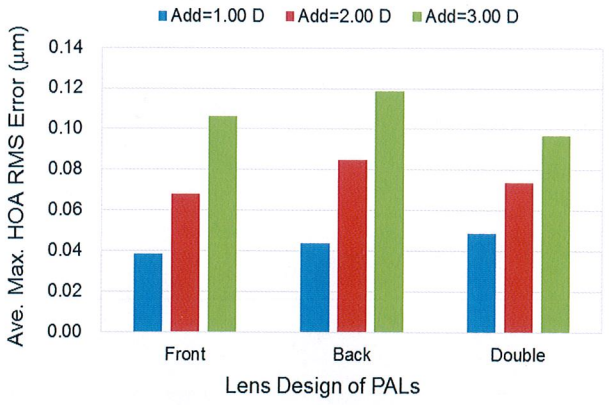

Fig. 10. Effect of add power and lens design on the HOA RMS errors of PALs.

design tend to have lower HOAs than the other two single-surface progressive lens designs by about 0.01 to 0.02 μm, especially at higher add power. Moreover, PALs with the back progressive lens design tend to have the highest average maximum HOAs up to 0.12 μm for an add power of +3.00 D. It is also easy to see that the add power plays a more important role than the lens design on the HOAs.

C. Test Efficiency of CMMs

The average measuring time spent by the surface sweeping CMM method with a five-axis probing system is less than 5 minutes to yield about 65,000 samples per surface scanning. Originally, it took about 16 hours for 12,100 measurements per surface using the traditional touch trigger point-type CMM method [16]. Even for a three-axis continuous scan type CMM system, it still took 30 minutes to complete a surface scanning measurement [22]. Therefore, compared with traditional touch trigger point-type CMM method, the test efficiency of the surface sweeping CMM is much better and around 200 times faster.

However, the measuring time is still longer than that for an optical measuring system such as the Rotlex Class Plus lens analyzer which is a moiré interferometer and only takes less than 2 minutes for a lens measurement [16]. Although the test efficiency is lower, the kind of lens design (front, back, or both) can only be determined by using CMM technology, which makes it unique and non-replaceable. From this work, it has been demonstrated that this advanced CMM technology with a revolutionary measuring head and sweeping probe system can be applied to optical lenses to gather large quantities of accurate inspection data at ultra-high scanning speeds with five-axis motion capability. The lens designs of PALs have been clearly distinguished. Moreover, through continuous improvement in hardware and software, the surface sweeping CMM could become more efficient and comparable to the optical measuring systems in terms of time

taken.

It is also worthwhile to note the limitation of the CMM surface measurements since they don't truly represent "as worn" power. In this paper, our analysis treats both surfaces equally, but when worn, the back surface is closer to the eye than the front surface [18]. Additionally, the PAL is normally tilted in front of the eye when worn, which might enhance the power differences between the measuring and "as worn" conditions due to the pantoscopic or face-form tilt.

Conclusions

The optical properties of progressive addition lenses (PALs) can be evaluated by using a non-optical surface sweeping coordinate measuring machine (CMM) with a five-axis probing system through the measurement of lens surface heights. The maximum power rate and root mean square (RMS) of HOAs in PALs increase with increasing add, but minimum 1.00-DC corridor width decreases with increasing add for all types of lens designs. On average, PALs with freeform both-surface lens design tend to have lower power rate and HOAs as well as wider progressive corridors than the single-surface progressive lens designs.

Compared with the traditional touch trigger point-type CMM method, the five-axis surface sweeping CMM method could greatly reduce measuring time to enable users to achieve previously unobtainable levels of inspection, which makes it become more comparable to the optical measuring methods.

Funding. Ministry of Science and Technology, Taiwan (MOST) (MOST 103-2320-B-212-002).

Acknowledgment. The author is grateful to the Renishaw (Taiwan) Inc. for supporting the surface sweeping CMM with REVO five-axis probing system and would like to thank Sean Lin (林厚君) for measurement, Saurabh Vishal and Mark A. Bullimore for many fruitful discussions and editorial assistance.

REFERENCES

1. P. Simonet, Y. Papineau, R. Lapointe, "Peripheral power variations in progressive addition lenses," Am. J. Optom. Physiol. Opt. 63, 873–880 (1986).
2. D. A. Atchison, "Optical performance of progressive power lenses," Clin. Exp. Optom. 70, 149–155 (1987).
3. J. E. Sheedy, M. Buri, I. Bailey, J. Azus, I. Borish, "Optics of progressive addition lenses," Am. J. Optom. Physiol. Opt. 64, 90–99 (1987).
4. C. Fowler, C. Sullivan, "Automatic measurement of varifocal spectacle lenses," Ophthalmic Physiol. Opt. 10, 86–89 (1990).
5. C. Fowler, "Technical note: apparatus for comparison of progressive addition spectacle lenses," Ophthalmic Physiol. Opt. 26, 502–506 (2006).
6. W. M. Rosenblum, D. K. O'LEARY, W. J. BLAKER, "Computerized Moire Analysis of Progressive Addition Lenses," Optom. Vis. Sci. 69, 936–940 (1992).
7. R. Bavli, "Wavefront sensing and processing using Moiré deflectometry," MAFO Ophthal Labs Indus 7, 30–32 (2010).
8. J. E. Sheedy, "Progressive addition lenses—matching the specific lens to patient needs," Optometry 75, 83–102 (2004).
9. J. E. Sheedy, R. F. Hardy, "The optics of occupational progressive lenses," Optometry 76, 432–441 (2005).
10. J. Sheedy, R. F. Hardy, J. R. Hayes, "Progressive addition lenses—measurements and ratings," Optometry 77, 23–39 (2006).
11. S. Chamadoira, R. Blendowske, E. Acosta, "Progressive addition lens measurement by point diffraction interferometry," Optom. Vis. Sci. 89, 1532–1542 (2012).
12. E. A. Villegas, P. Artal, "Comparison of aberrations in different types of progressive power lenses," Ophthalmic Physiol. Opt. 24, 419–426 (2004).

13. E. A. Villegas, P. Artal, "Visual acuity and optical parameters in progressive-power lenses," Optom. Vis. Sci. 83, 672–681 (2006).
14. C. Zhou, W. Wang, K. Yang, X. Chai, Q. Ren, "Measurement and comparison of the optical performance of an ophthalmic lens based on a Hartmann-Shack wavefront sensor in real viewing conditions," Appl. Opt. 47, 6434–6441 (2008).
15. J. Yu, F. Fang, and Z. Qiu, "Aberrations measurement of freeform spectacle lenses based on Hartmann wavefront technology," Appl. Opt. 54, 986–994 (2015).
16. C. Y. Huang, T. W. Raasch, Y. Y. Allen, J. E. Sheedy, B. Andre, and M. A. Bullimore, "Comparison of three techniques in measuring progressive addition lenses," Optom. Vis. Sci. 89, 1564–1573 (2012).
17. T. W. Raasch, L. Su, A. Yi, "Whole-surface characterization of progressive addition lenses," Optom. Vis. Sci. 88, E217–E226 (2011).
18. C. Y. Huang, T. W. Raasch, Y. Y. Allen, M. A. Bullimore, "Comparison of progressive addition lenses by direct measurement of surface shape," Optom. Vis. Sci. 90, 565–575 (2013).
19. J. Hadaway, R. Chipman, J. Drewes, T. Hargrove, "The Spectacle Lens Image Quality Mapper," in OSA Technical Digest Series: Vision Science and Its Applications, Optical Society of America, 206–209 (1999).
20. D. Mazuet, "Progressive addition lenses and commercial instruments limitations," in OSA Technical Digest Series: Vision Science and Its Applications, Optical Society of America, 179–182 (2001).
21. H. Herman, "How to control your freeform process comparison of 3 measurement methods," MAFO 2, 26–28 (2010).
22. C.-Y. Huang, "Evaluation of progressive addition lenses by sliding-type coordinate measuring technique," in Optics & Photonics Taiwan International Conference (OPTIC), (2013).
23. G. McFarland, K. B. Jonas, "Surface sensing device with optical sensor," US Patent 7,847,955 B2, (2010).
24. G. McFarland, K. C. H. Nai, N. J. Weston, I. W. McLean, "Method for scanning the surface of a workpiece," US Patent 8,006,398 B2, (2011).
25. G. McFarland, K. B. Jonas, "Surface sensing device with optical sensor," US Patent 8,144,340 B2, (2012).
26. G. McFarland, K. C. H. Nai, N. J. Weston, I. W. McLean, "Probe head for scanning the surface of a workpiece," US Patent 8,978,261 B2, (2015).
27. K. Mamour, "Renscan5 and REVO® – technology and applications," (2008). Permission from Renishaw for the use of the figure.
28. T. Raasch, "Aberrations and spherocylindrical powers within subapertures of freeform surfaces," JOSA A 28, 2642–2646 (2011).